Fatigue of weld ends under combined in- and out-of-phase multiaxial loading

E. Shams
Technische Universität Darmstadt, Materials Mechanics Group, Franziska-Braun-Str. 3, D-64287 Darmstadt, Germany
shams@wm.tu-darmstadt.de

M. Vormwald
Technische Universität Darmstadt, Materials Mechanics Group, Franziska-Braun-Str. 3, D-64287 Darmstadt, Germany
vormwald@wm.tu-darmstadt.de

ABSTRACT. Weld start and end points are fatigue failure sensitive locations. Their fatigue behaviour especially in thin sheet structures under multiaxial load conditions is not sufficiently explored so far. Therefore, a research project was initiated to increase the knowledge concerning this topic, which is of special interest in the automotive industry. In the present study, fatigue tests on welded joints were conducted. In the numerical part of the study, notch stresses were calculated with an idealised weld end model. A numerical method which combines the geometrical and statistical size effect to an integrated approach was used, in order to consider the size effects.

KEYWORDS. Weld ends; Fatigue; Notch stress; Size effect; Multiaxial.

Citation: Shams, E., Vormwald, M., Fatigue of weld ends under combined in- and out-of-phase multiaxial loading, Frattura ed Integrità Strutturale, 38 (2016) 114-120.

Received: 18.05.2016
Accepted: 15.06.2016
Published: 01.10.2016

Copyright: © 2016 This is an open access article under the terms of the CC-BY 4.0, which permits unrestricted use, distribution, and reproduction in any medium, provided the original author and source are credited.

INTRODUCTION

Welded structures often contain weld start and end points, which are the critical location for the failure. Normally, fatigue design of welded components proceeds from *S–N* curves (fatigue strength versus number of cycles). Concerning weld start and end points, the knowledge of *S-N* curve parameters is limited to either normal [1-5] or shear [6] stressed structures. In these investigations, dealing only with uniaxial loading conditions, geometrically idealised weld end models with concept radii of r_{normal} = 0.20 mm respectively r_{shear} = 0.05 mm were created. These models base on the real weld geometry obtained by means of high-precision 3D-scanner. In connection with these models, recommendations for determining notch stresses by applying the finite element (FE) method were developed. Nowadays, different *S-N* curves are assigned to weld toe and weld root failure scenarios induced by normal and shear stresses.

Further studies have shown, that an evaluation of both stress gradient and expansion of the notch area realizes the standardisation of *S-N* curves belonging to various structural shapes and sizes [4-5]. In the framework of the "Numerical Method regarding Size Effects for Standardisation of Wöhler curves" (NuMeSiS), a standardised stress is to be derived by

consideration of geometrical and statistical size effects. In the first step of this method, the effective stress distribution over an area to be investigated according to Neuber [7] is to be determined. Next, the highly stressed surface based on the effective stress distribution is calculated using the weakest link model according to Weibull [8].
Many research activities have been initiated during the last years for the investigation of fatigue design of multiaxially loaded welded joints [9-11]. Vormwald [12] explored in the event of variable amplitude loading conditions a list of challenges have to be considered. Nevertheless, the case of weld ends under such loading is not sufficiently explored yet. However, the application of the method NuMeSiS opens up the possibility to standardise the *S-N* curves belonging to various weld shapes and loading conditions.
In the present paper, the fatigue behaviour of weld ends under combined in- and out-of-phase multiaxial loading in thin sheet structures, which is of special interest in the automotive industry, is addressed. In the experimental part of this research, cycles to rupture at different stress amplitudes were derived from fatigue testing. Due to the complex geometry of weld ends, the notch stress concept was used in order to assess the multiaxial stress-states based on an idealised weld end model.

EXPERIMENTAL INVESTIGATION

Specimens and Testing

Fatigue tests on MAG-welded tube-tube joints from fine-grained and engineering steels (S340+N and E355+N) under constant amplitude loading in the range of 10^4 to $5 \cdot 10^6$ cycles to rupture were conducted. Any effect of residual welding stresses is excluded because all the specimens were stress-relieved by heat treatment prior to testing. The 490 mm long test specimen consists of two tubes with an overlap length of 60 mm. Two seam welds at opposing quadrants joined the two tubes, see Fig. 1. The sheet thicknesses of the inner and outer tubes are t_1 = 2.0 mm and t_2 = 2.5 mm.

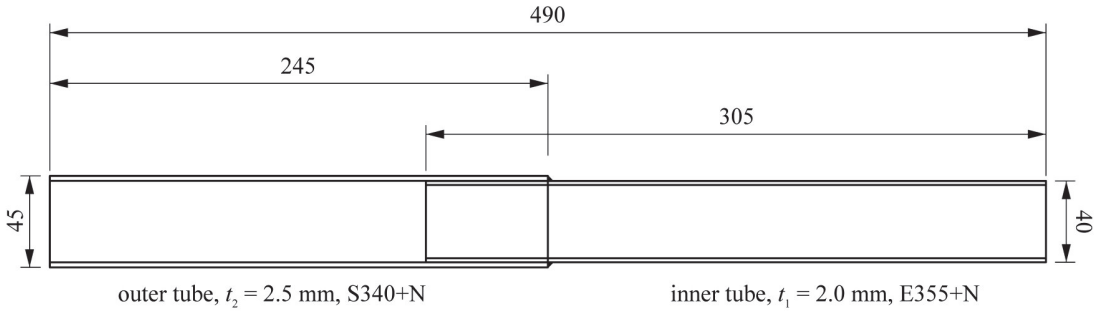

Figure 1: Overlapped tube-tube specimen.

For the experimental investigations eight different loading types, shown in Fig. 2, were considered. The specimens were subjected to both alternating and pulsating pure axial force, pure torsional moment and proportional as well as non-proportional combinations of both loadings. In the latter case the phase shift was set at 90°. The selected ratio of the torsional moment to the axial force stress amplitudes of the combined loading was $M_{T,a}$ / $F_{\perp,a}$ = 28 Nm/kN. This is the ratio between the torsional moment and axial force amplitudes both led to $1 \cdot 10^6$ cycles to rupture in uniaxial tests. The experiments have been conducted using a servo-hydraulic multiaxial test rig with testing frequencies of 8-10 Hz for uniaxial and 1-2 Hz for multiaxial loading conditions.
During testing, the fatigue cracks were monitored by taking photographs of the four existing weld start and end points at predefined numbers of cycles. Prior to testing, the specimens were sprayed using a scan spray, in order to ease the optical detectability of both formation and growth of the fatigue cracks after the test. The experimental set-up is depicted in Fig. 3 on the left hand side.

Results

Typical failures of specimens under pulsating uni- and multiaxial loading are shown in Fig. 3 on the right hand side. In all of the tested specimens fatigue cracks initiated at the transition area between weld toe and root, either at the weld start or at the weld end position. In the case of specimens under pure axial loading, the fatigue cracks were initiated in both the weld start and end locations. The crack fronts propagated to each other at the weld toe on the outer tube side during

cyclic loading and finally merged to one crack, Fig. 3 (a). In specimens subjected to torsional moment, the cracks propagated to the inner and outer tube halves, Fig. 3 (b). In the case of combined in-phase loading, the fatigue cracks propagated either into the outer pipe or through the weld metal, Fig. 3 (c). On the contrary, the welds failed only with crack propagation through the weld metal, when force and moment were phase shifted by 90°, Fig. 3 (d).

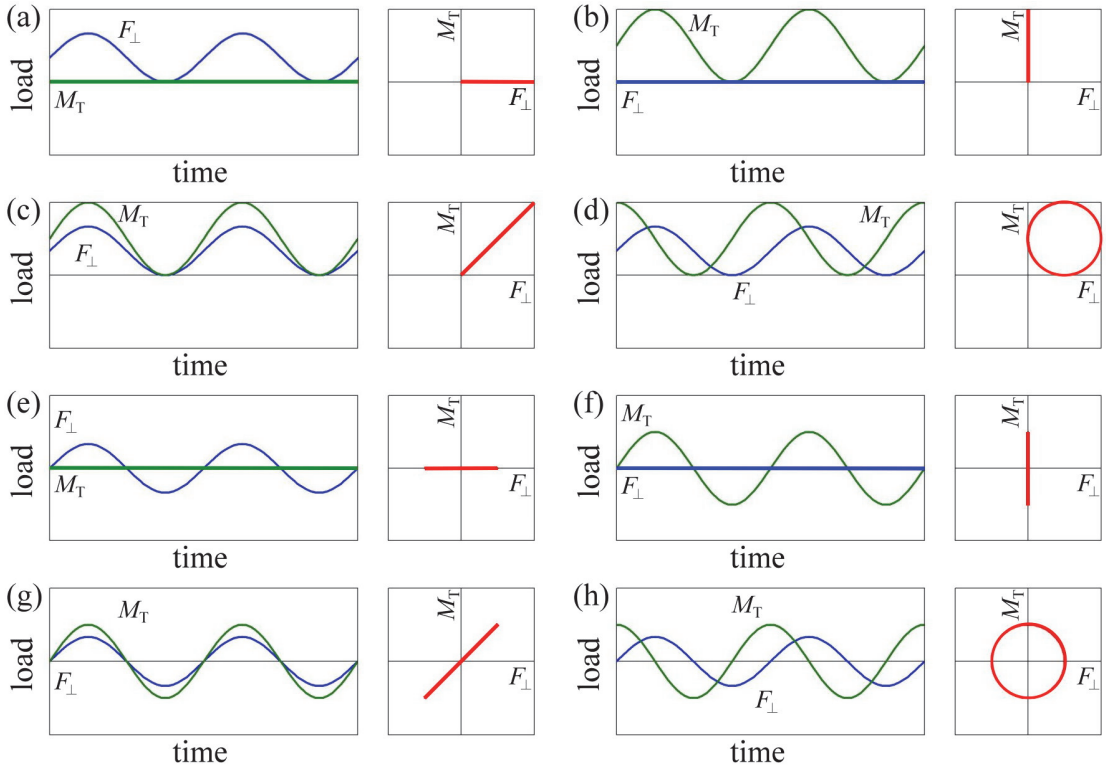

Figure 2: Loading types: (a) pure axial force, $R = 0$, (b) pure tosional moment, $R = 0$, (c) proportional, $R = 0$, (d) non-proportional, $R = 0$, (e) pure axial force, $R = -1$, (f) pure tosional moment $R = -1$, (g) proportional, $R = -1$, (h) non-proportional, $R = -1$.

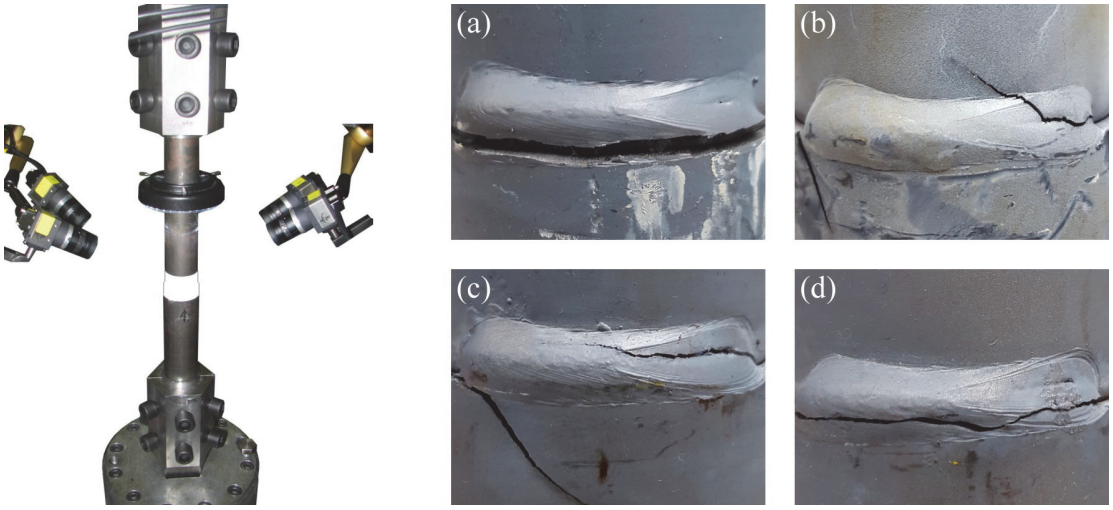

Figure 3: Experimental set-up (left); Failure modes of welded joints under axial force (a), torsional moment (b) and proportional (c) as well as non-proportional (d) combinations (right).

The results are presented in Figs. 4 and 5 in the form of *S-N* curves. Regression lines are added for a 50% probability of survival, for pulsating and alternating loading respectively. The slopes of the *S-N* curves vary in the range of 3.7 to 5.7. The experiments revealed a significant difference between in- and out-of-phase combined loadings only at load levels with $N < 10^5$ and in case of alternating loading.

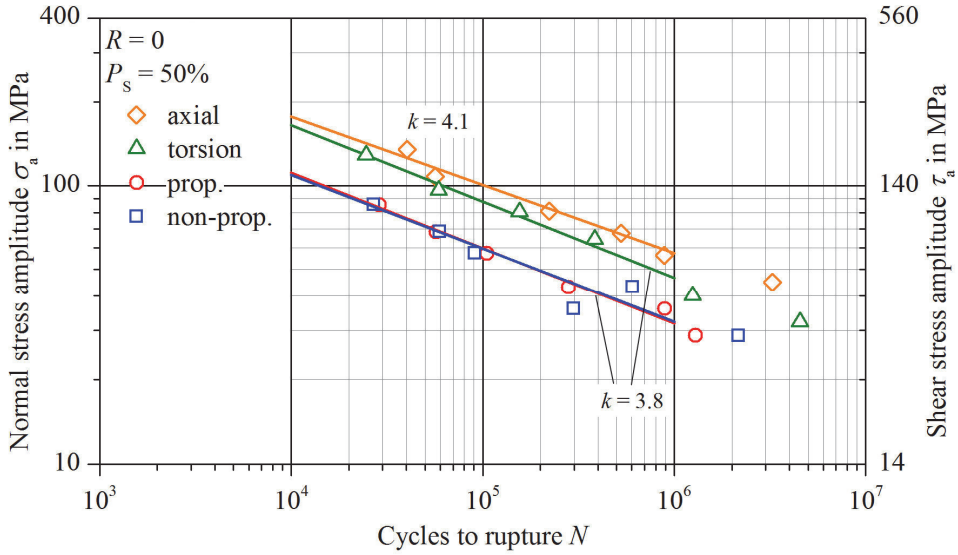

Figure 4: *S-N* curves for pulasting loading.

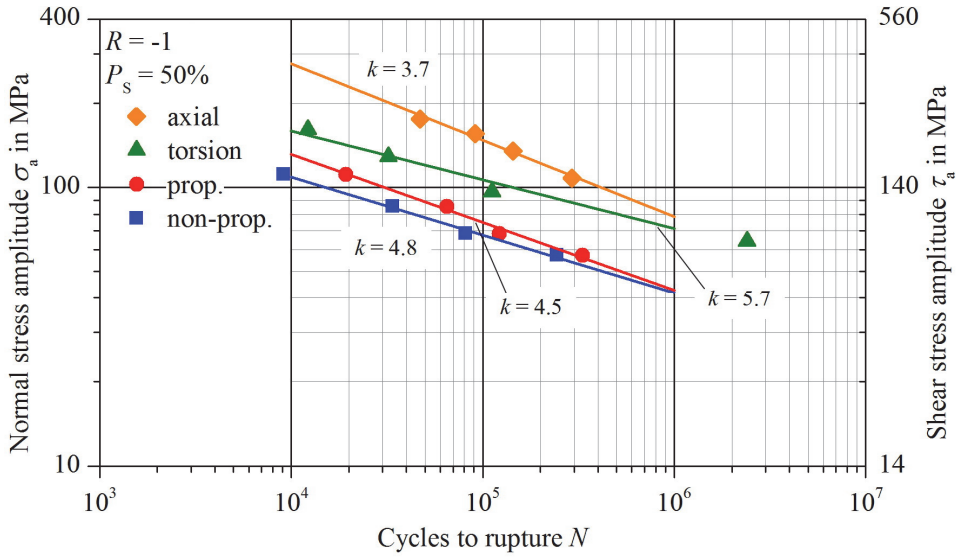

Figure 5: *S-N* curves for alternating loading.

NUMERICAL ANALYSES

Notch Stresses and Size Effects

In the numerical part of the study, notch stresses were calculated with an idealised weld end geometry. The modelling steps of such an idealised weld end geometry are comprehensively described in [1-6]. A submodelling technique has been used, in order to calculate the von Mises equivalent stresses. The geometry of the submodel takes as a basis a

radius of r_{root} = 0.05 mm at the weld root and a radius of r_{toe} = 0.2 mm at the weld toe, Fig. 6 left. The solid FE-model, as shown in Fig. 6 right, is represented as a mesh of tetrahedral elements with a quadratic shape function. It incorporates linear elastic material behaviour.

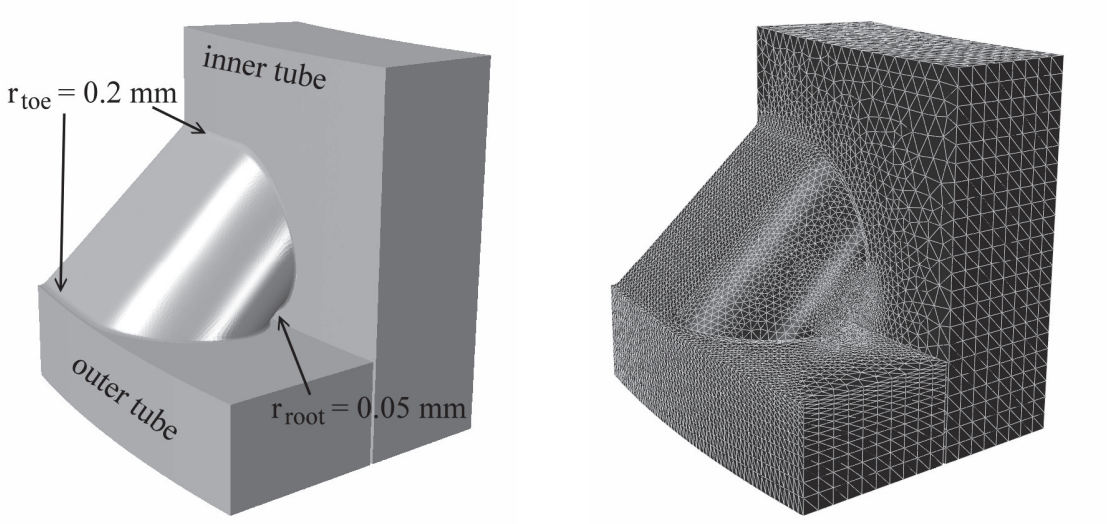

Figure 6: Geometry of the submodel (left); FE-modell(right).

The numerical method NuMeSiS was used, in order to consider the size effects in the post-processing stage of the FE analysis. Within this method, first the effective stress for each node $\sigma_{\rho^*,\psi}$ on the surface first to be selected has to be calculated by integrating the elastic stress distribution over the micro structural length ρ^* in direction of the highest stress gradient. The highly stressed surface results by summation based on the calculated effective stresses, which leads to a standardised stress $\sigma_{\rho^*,\kappa}$ as shown in Eq. 1. Herein, A_ψ represents the corresponding surface to the node ψ.

$$\sigma_{\rho^*,\kappa} = \left(\sum_{\psi} (\sigma_{\rho^*,\psi})^{\kappa} \cdot \frac{A_\psi}{I_{A,ref}} \right)^{\frac{1}{\kappa}} \tag{1}$$

Furthermore, the micro structural length ρ^*, the Weibull exponent κ and the highly stressed reference surface $I_{A,\mathrm{ref}}$ are concept-tied parameters, the first two also material parameters, and have been set in [4-5] to values as stated below:

ρ^*	κ	$I_{A,\mathrm{ref}}$
0.4 mm	9	0.2 mm²

Table 1: Concept parameters.

Non-proportional Loading

An automated analysis algorithm for applying this method for different loading configurations has been produced. In the case of non-proportional loading, the change in the von Mises stresses inside a load cycle has to be calculated, which remain always positive due to square root extraction. Therefore, the sign of either normal force or torsional moment has to be assigned to the calculated positive stresses. Now, the equivalent stress amplitude $\sigma_{v,\psi,a}$ can be determined using the unsteady development of the stresses from the half difference between the extreme values at each node. Note that the effective stresses $\sigma_{\rho^*,\psi,a}$ over the surface nodes do not belong necessarily to the same time. Finally, the stress amplitude $\sigma_{\rho^*,\kappa,a}$ including the size effects is derived by using Eq. 1.

Results

To standardise the *S-N* curves belonging to different load ratios, the influence of the mean stresses was considered through the fatigue enhancement factor $f(R)$ according to IIW recommendations [13]. The fatigue lives of all tested loading configurations are related to the standardised stress values in Fig. 7. The failure criterion is the specimen rupture. Regression analysis leads to the life curve (solid line in Fig. 7), having a slope of $k = 3.0$ and a scatter value of $T_\sigma = 1{:}2.0$. The scatter band for 10% and 90% probabilities of survival is illustrated with dashed curves.

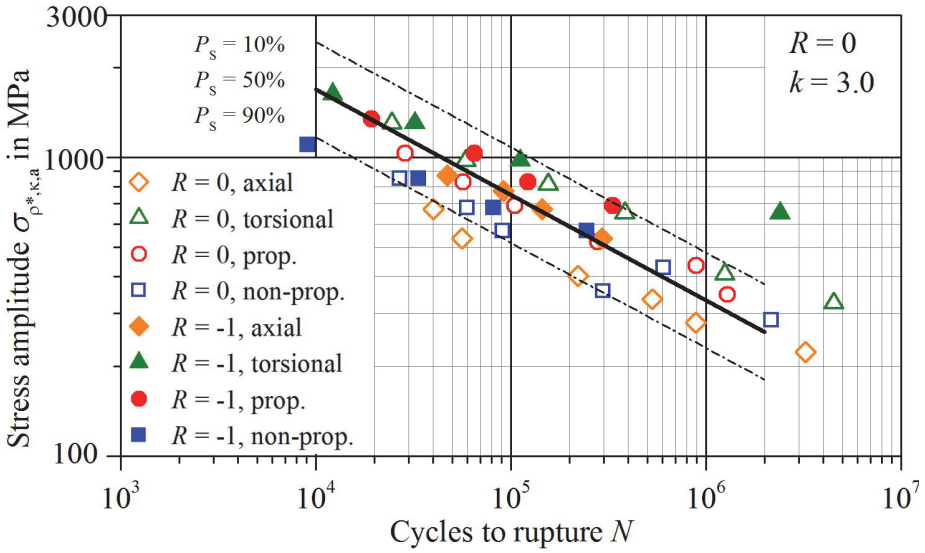

Figure 7: Standardised *S-N* curve.

Conclusions

A general approach for the fatigue assessment of weld ends under multiaxial loading has been developed. Notch stresses have been calculated based on an idealised weld end model including different radii for weld root and toe. The final result is a *S-N* curve for the determination of fatigue life of weld ends under multiaxial loading conditions.

Acknowledgements

The authors gratefully acknowledge the financial support of the research Project A 288 by the "Research Association for the Iron and Metalworking Industry e. V." and the "Foundation Research on Steel Application". Technical support during the project was given by the Research Association of Automotive Technology FAT. The specimens were provided by "Benteler Automobiltechnik GmbH" and the support is highly appreciated.

References

[1] Kaffenberger, M., Vormwald, M., Application of the notch stress concept to the real geometry of weld end points, Mat.-wiss. u. Werkstofftech., 42 (2011) 289-297.

[2] Kaffenberger, M., Vormwald, M., Fatigue resistance of weld ends - Analysis of the notch stress using real geometry, Mat.-wiss. u. Werkstofftech., 42 (2011) 874-880.

[3] Kaffenberger, M., Malikoutsakis, M., Savaidis, G., Vormwald, M., Fatigue resistance of weld ends, Comput. Mater. Sci., 52 (2012) 287-292.

[4] Kaffenberger, M., Vormwald, M., Considering size effects in the notch stress concept for fatigue assessment of welded joints, Comput. Mater. Sci., 64 (2012) 71-78.

[5] Kaffenberger, M., Vormwald, M., Schwingfestigkeit von Schweissnahtenden und Übertragbarkeit von Schweissverbindungswöhlerlinien, Mater. Test., 55 (2013) 553-560.
[6] Shams, E., Malikoutsakis, M., Savaidis, G., Vormwald, M., Notch stress and fracture mechanics based assessment of fatigue of seam weld ends under shear loading, Fatigue Fract. Eng. Mater. Struct., 37 (2014) 740-750.
[7] Neuber, H., Über die Berücksichtigung der Spannungskonzentration bei Festigkeitsberechnungen, Konstruktion, 20-7 (1968) 245-251.
[8] Weibull, W., Zur Abhängigkeit der Festigkeit von der Probengröße, Ingenieur-Archiv, 28 (1959) 360-362.
[9] Sonsino, C.M., Multiaxial fatigue of welded joints under in-phase and out-of-phase local strains and stresses, Int. J. Fatigue, 17 (1995) 55-70.
[10] Eibl, M., Sonsino, C.M., Kaufmann, H., Zhang, G., Fatigue assessment of laser welded thin sheet aluminium, Int. J. Fatigue, 25 (2003) 719-731.
[11] Wiebesiek, J., Störzel, K., Bruder, T., Kaufmann, H., Multiaxial fatigue behaviour of laserbeam-welded thin steel and aluminium sheets under proportional and non-proportional combined loading, Int. J. Fatigue, 33 (2011) 992-1005.
[12] Vormwald, M., Multi-challenge aspects in fatigue due to the combined occurrence of multiaxiality, variable amplitude loading, and size effects, Frattura ed Integrità Strutturale, 33 (2015) 253-261.
[13] Hobbacher, A.F., Recommendations for Fatigue Design of Welded Joints and Components, Springer, Switzerland, (2016).